Aldose Reductase Inhibition Prevents Development of Posterior Capsular Opacification in an In Vivo Model of Cataract Surgery

Leonid M. Zukin,[1] Michelle G. Pedler,[1] Sergio Groman-Lupa,[1,2] Mina Pantcheva,[1] David A. Ammar,[1] and J. Mark Petrash[1,3]

[1]Department of Ophthalmology, University of Colorado, Anschutz Medical Campus, Aurora, Colorado, United States
[2]Asociación para Evitar la Ceguera en México, Mexico City, Mexico
[3]Department of Pharmaceutical Sciences, Skaggs School of Pharmacy and Pharmaceutical Sciences, University of Colorado, Anschutz Medical Campus, Aurora, Colorado, United States

Correspondence: J. Mark Petrash, Mail Stop 8311, RC1-North, 12800 E. 19th Avenue, Room P18-5100, Aurora, CO 80045, USA; mark.petrash@ucdenver.edu.

Submitted: January 31, 2018
Accepted: June 12, 2018

Citation: Zukin LM, Pedler MG, Groman-Lupa S, Pantcheva M, Ammar DA, Petrash JM. Aldose reductase inhibition prevents development of posterior capsular opacification in an in vivo model of cataract surgery. *Invest Ophthalmol Vis Sci*. 2018;59:3591–3598. https://doi.org/10.1167/iovs.18-23935

Purpose. Cataract surgery is a procedure by which the lens fiber cell mass is removed from its capsular bag and replaced with a synthetic intraocular lens. Postoperatively, remnant lens epithelial cells can undergo an aberrant wound healing response characterized by an epithelial-to-mesenchymal transition (EMT), leading to posterior capsular opacification (PCO). Aldose reductase (AR) inhibition has been shown to decrease EMT markers in cell culture models. In this study, we aim to demonstrate that AR inhibition can attenuate induction of EMT markers in an in vivo model of cataract surgery.

Methods. A modified extracapsular lens extraction (ECLE) was performed on C57BL/6 wildtype, AR overexpression (AR-Tg), and AR knockout mice. Immunofluorescent staining for the myofibroblast marker α-smooth muscle actin (α-SMA), epithelial marker E-cadherin, and lens fiber cell markers αA-crystallin and Aquaporin 0 was used to characterize postoperative PCO. Quantitative reverse transcription PCR (qRT-PCR) was employed to quantify postoperative changes in α-SMA, vimentin, fibronectin, and E-cadherin. In a separate experiment, the AR inhibitor Sorbinil was applied postoperatively and qRT-PCR was used to assess changes in EMT markers.

Results. Genetic AR knockout reduced ECLE-induced upregulation of α-SMA and downregulation of E-cadherin. These immunofluorescent changes were mirrored quantitatively in changes in mRNA levels. Similarly, Sorbinil blocked characteristic postoperative EMT changes in AR-Tg mice. Interestingly, genetic AR knockout did not prevent postoperative induction of the lens fiber cell markers αA-crystallin and Aquaporin 0.

Conclusions. AR inhibition prevents the postoperative changes in EMT markers characteristic of PCO yet preserves the postoperative induction of lens fiber cell markers.

Keywords: aldose reductase, EMT, PCO, cataractogenesis

Posterior capsular opacification (PCO), or secondary cataract, is a common complication of cataract surgery, occurring in up to 20% to 30% of patients postoperatively.[1] Cataract surgery involves removal of a majority of the fiber cell mass of the lens held within the lens capsular bag, and subsequent implantation of a synthetic intraocular lens (IOL) to restore visual clarity. While cataract extraction eliminates most lens tissue, some lens epithelial cells (LECs) inevitably remain attached to the inner surface of the capsular bag. In response to the trauma of cataract surgery, these residual LECs undergo an aberrant wound healing response characterized by proliferation, transdifferentiation to a myofibroblast phenotype, and migration toward the posterior capsule, where they cause wrinkling and fibrosis of the normally smooth capsule and consequent disruption of visual axis clarity.[2] Improvements in surgical tools and techniques, together with the introduction of new IOL materials and structural design, have lowered but not eliminated the incidence of PCO worldwide.[3] To date no inhibitors have been approved to block the onset and progression of PCO at the cellular level.

Transforming growth factor-β (TGF-β) is considered a central regulator of PCO through its role in inducing epithelial-to-mesenchymal transition (EMT) of LECs.[2] One of the key TGF-β signaling transduction pathways involves SMAD proteins,[4–6] which convey information from the TGF-β receptor, leading to the formation of spindle-like myofibroblast cells[7] and expression of EMT markers, including α-smooth muscle actin (α-SMA), fibronectin, and vimentin.[8–12] This important signaling link in ocular tissues has been demonstrated through experiments showing cataract induction in lenses cultured in the presence of TGF-β.[13] Furthermore, inhibiting TGF-β/SMAD signaling abrogates EMT and therefore PCO.[14]

Recent studies have suggested that aldose reductase (AR) also plays a critical role in the development of PCO. AR is well known for its role in the pathogenesis of various secondary complications of diabetes mellitus through its enzymatic function in converting glucose to sorbitol in the polyol

pathway. As a key enzyme in the polyol pathway, AR is also thought to contribute to formation of reactive oxygen species (ROS) via three mechanisms: depletion of antioxidant molecules like NADPH and GSH, generation of NADH (which can lead to superoxide anion formation), and increased production of potent nonenzymatic glycation agents, which can increase ROS levels by creating advanced glycation end-products.[15] ROS in ocular tissues have been shown to cause LEC growth and a PCO-like phenotype.[16] Furthermore, various antioxidant agents, like caffeic acid and retinoic acid, have shown the potential to prevent this phenotype.[17–19] Importantly, AR inhibition has been shown to suppress ROS production in ocular tissues.[20–22] The critical link between AR and PCO is further substantiated by studies demonstrating that AR overexpression leads to induction of EMT and PCO biomarkers[23] and that AR inhibition can decrease these markers.[24] Indeed, AR has been hypothesized as a druggable target for prevention of cataracts and oxidative damage in diabetes.[25–27]

Recently, we showed that TGF-β–mediated EMT and LEC migration can be disrupted through inhibition of AR in a cell culture model.[21] This demonstrated an important regulatory relationship between AR and TGF-β signaling and suggested that AR inhibition could be a possible therapeutic strategy against PCO development. To further explore AR as a drug target for PCO prevention, it is important to demonstrate similar findings with an in vivo mouse model of cataract surgery. This facilitates more complete modeling of PCO characteristics and the ocular inflammatory response.[28] In this study, we demonstrate that inhibition of AR, both pharmacologically and via genetic knockdown, can attenuate the induction of EMT markers in an in vivo model of cataract surgery.

Methods

Transgenic Mice

All experiments were conducted in accordance with the ARVO Statement for the Use of Animals in Ophthalmic and Vision Research and were approved by the University of Colorado Institutional Animal Care and Use Committee. C57BL/6 wild-type (WT) mice were acquired from The Jackson Laboratory (Bar Harbor, ME, USA). The Par40 strain of AR transgenic mice (AR-Tg) and the AR knockout strain (ARKO) were generated as in previous studies.[29–31]

Model Cataract Surgery

Cataract surgery was modeled in mice using a modified extracapsular lens extraction technique (ECLE) based on previously published techniques.[32–34] Adult mice were anesthetized with 80 mg/kg ketamine and 5 mg/kg Xylazine. One eye of each mouse was dilated using several drops of topical phenylephrine and tropicamide. A 1- to 1.5-mm central corneal incision was made using a disposable ophthalmic knife. Following reinflation of the anterior chamber with an ophthalmic viscoelastic agent, a similarly sized incision was made in the anterior capsule. A viscoelastic cannula was used to instill saline into the capsular space to hydro-dissect the lens fiber mass away from the capsule. Angled jeweler forceps were used to remove the lens mass by applying gentle pressure near the equator of the eye. After the lens mass was expelled, careful irrigation of the capsule was performed to remove any residual lens material (in particular, the lens cortex). A viscoelastic agent was then injected into the capsule and anterior chamber to reinflate the eye and maintain its structural integrity postoperatively. The corneal incision was closed using 10-0 nylon sutures. Animals were euthanized 5 days postoperatively and lenses removed from both the surgical eye as well as the contralateral eye, which served as an experimental control. For analysis, whole eyes from ECLE experiments were preserved for immunofluorescence. In some cases, capsular bags were microdissected from the eye and used for isolation of RNA for PCR measurements. Surgery, euthanasia, and dissection were performed in parallel for each experiment to ensure consistency and comparability. Furthermore, the surgeon was blinded to the genetic strain of each mouse during operations. For experiments involving treatment with Sorbinil ([4S]-6-Fluoro-2,3-dihydro-spiro[4H-1-benzopyran-4,4′-imidazolidine]-2′,5′-dione), mice were injected intraperitoneally with 10 mg/kg at the time of surgery followed by twice daily injections on postoperative days 1 through 5. Sorbinil was provided by Pfizer Central Research (Groton, CT, USA). Vehicle controls contained 1X phosphate buffered saline.

Immunofluorescence

Postoperative eyes were fixed in 4% paraformaldehyde for 30 minutes, then transferred to 1X phosphate buffered saline solutions of increasing sucrose concentration (10% for four hours, 20% for four hours, and 30% overnight). Tissues were then embedded in optimal cutting temperature (OCT) media (Tissue Tek, Torrance, CA, USA) and frozen to −80°C before being cut into 10-µm thick sections using a cryostat (Microm HM550; Thermo Fisher Scientific, Waltham, MA, USA). Sections were placed onto glass slides, fixed in acetone at −20°C, and blocked in 5% bovine serum albumin with 0.4% Triton X-100 for 30 minutes at room temperature. Samples were incubated with primary antibodies as outlined in the Table below. After washing slides three times with 1X phosphate buffered saline, samples were incubated with a 1:200 dilution of species appropriate secondary anti-IgG conjugated to AlexaFluor 488 (Thermo Fisher Scientific) for 30 minutes at room temperature. Slides were washed three times, covered with antifade mounting media (Vector Laboratories, Burlingame, CA, USA) containing 4′,6-diamidion-2-phenylindole (DAPI), and coverslipped. Experiments were repeated at least three times on each mouse strain using appropriate internal controls for staining. The slides were imaged using a confocal microscope (Eclipse Ti; Nikon Corp., Tokyo, Japan). All processing was performed in parallel for each experiment/figure. Furthermore, all imaging parameters (including laser intensity and brightness) were held constant within each experiment. All immunofluorescence images present in this study came from the same set of mice, with different stains applied to nearly consecutive tissue sections.

Quantitative (q)RT-PCR

Following dissection of capsular bags from postsurgical and control eyes, RNA was isolated (RNeasy Microarray Tissue Mini Kit; Qiagen, Austin, TX, USA) according to the manufacturer's protocol. Complementary DNA was synthesized using a cDNA synthesis kit for qRT-PCR (iScript Advance; Bio-Rad Laboratories, Hercules, CA, USA). For qRT-PCR, we used a SYBR green supermix (iTaq Universal SYBR Green Supermix; Bio-Rad Laboratories) according to the manufacturer's instructions on a qRT-PCR detection system (CFX Connect; Bio-Rad Laboratories). The primers used in this study (Integrated DNA Technologies, Coralville, IA, USA) were α-SMA (forward 5′-CTGTTATAGGTGGTTTCGTGGA-3′; reverse 5′-GAGCTA CGAACTGCCTGAC-3′), fibronectin (forward 5′-TTGTTCGT AGACACTGGAGAC-3′; reverse 5′-GAGCTATCCAATTTCACCT TCAG-3′), vimentin (forward 5′-TCAACATCCTGTCTGACTG-3′; reverse 5′-ATCAGCTCACCAACGACAAG-3′), and E-cadherin

Table. List of Primary Antibodies Used in This Study

Antibody	Dilution	Incubation	Product #, Company
α-SMA	1:500	1 hour at room temperature	ab32575, Abcam (Cambridge, MA, USA)
E-Cadherin	1:50	Overnight at 4°C	4065, Cell Signaling (Danvers, MA, USA)
αA-Crystallin	1:200	1 hour at room temperature	ADI-SPA-221, Enzo (Farmingdale, NY, USA)
Aquaporin 0	1:200	Overnight at 4°C	H-44, Santa Cruz (Dallas, TX, USA)

(forward 5′-AGTCTCGTTTCTTGTCTTCTGAG-3′; reverse 5′-GAGCTGTCTACCAAAGTGACG-3′). Glyceraldehyde 3-phosphate dehydrogenase (GAPDH) was used as an internal control (forward 5′-CTGGAGAACATGCCAAGTA-3′; reverse 5′-TGTTGCTGTAGCCGTATTCA-3′). Statistical analysis was performed with graphing software (GraphPad Prism; GraphPad Software, Inc., La Jolla, CA, USA) using the $2^{\Delta Ct}$ method. Data were analyzed by ANOVA with Tukey's post hoc test. Asterisks refer to P values according to the following: $^{*}P < 0.05$, $^{**}P < 0.01$, and $^{***}P < 0.001$.

Results

Genetic Knockout of AR Reduces ECLE-Induced Upregulation of the Myofibroblast Marker α-SMA

Previous research in lens epithelial cell cultures has demonstrated a link between AR inhibition and the attenuation of TGF-β2 induced expression of EMT and fibrosis markers (α-SMA, fibronectin, vimentin).[21] However, it is unclear whether this inhibition can lead to observable changes in protein expression or gross morphology in the in vivo situation. To test whether AR inhibition can prevent EMT and therefore PCO in an animal model, we used immunofluorescent staining to examine eyes of wild-type (WT), AR knockout (ARKO), and AR overexpression (AR-Tg) mice 5 days after extracapsular lens extraction surgery (ECLE). Immediately after surgery, a thin layer of anterior lens epithelial cells detected by DAPI staining was observed lining the anterior capsular bag in all three mouse strains: ARKO (Fig. 1A), WT (Fig. 1C), and AR-Tg (Fig. 1E). There was very little staining for the myofibroblast marker α-SMA observed immediately after surgery (Figs. 1A, 1C, 1E). Five days postoperatively, ARKO mice exhibited mild α-SMA staining mostly concentrated to a thin layer of cells lining the anterior capsule and, to a lesser extent, the posterior capsule (Fig. 1B). In WT mice, by contrast, α-SMA expression was present in a markedly thicker layer of cells lining both the anterior and posterior capsules (Fig. 1D). AR-Tg mice exhibited robust α-SMA expression postoperatively, with α-SMA positive cells filling the entire space of the capsular bag (Fig. 1F). Taken together, these data demonstrate that our modified ECLE procedure appropriately induced the fibrosis marker α-SMA in WT and, to a greater extent, AR-Tg mice. Furthermore, genetic knockdown of AR substantially abrogated this surgery-induced response.

Genetic Knockout of AR Reduces ECLE-Induced Downregulation of the Epithelial Marker E-Cadherin

Concomitant with induction of myofibroblast markers like α-SMA, EMT is characterized by down-regulation of epithelial markers

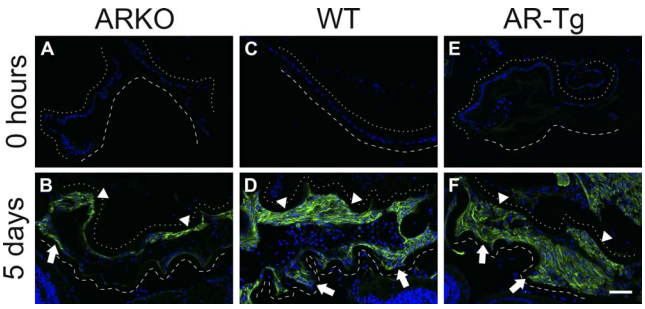

Figure 1. Expression of the myofibroblast marker α-SMA 0 hours and 5 days after cataract surgery in ARKO (**A**, **B**), WT (**C**, **D**), and AR-Tg (**E**, **F**) mice. Immediately after surgery, no α-SMA expression is seen within the remnant capsular bag in any strain, with only a thin layer of anterior lens epithelial cells present (**A**, **C**, **E**). Five days after surgery, all strains show α-SMA expression. However, ARKO (**B**) has appreciably less expression overall as compared to WT (**D**) and AR-Tg (**F**), with α-SMA being confined to a relatively thin layer along the capsular border. WT (**D**) has a much thicker layer of α-SMA deposition along the capsular border, but still lacks α-SMA expression connecting the anterior and posterior capsule. Unlike ARKO and WT, AR-Tg (**F**) displays robust α-SMA expression spanning the entire capsular bag space from the posterior capsule to the anterior capsule. All panels show α-SMA expression (*green*) along with nuclei (DAPI, *blue*). *Dotted line* traces the anterior capsule; dashed line traces the posterior capsule. *Arrowheads* denote α-SMA depositions along the anterior capsule, while *arrows* denote α-SMA deposits along the posterior capsule. *Scale bar*: 50 μm.

such as E-cadherin.[35] In a similar experiment as above, we performed immunostaining directed at E-cadherin. Immediately postoperatively, an E-cadherin positive layer of anterior lens epithelial cells is present lining the anterior capsule (Figs. 2A, 2C, 2E). Five days postoperatively, ARKO mice displayed persistent yet mildly attenuated E-cadherin expression in a thin cell layer lining the anterior and posterior capsule (Fig. 2B). WT mice, on the other hand, displayed markedly decreased E-cadherin expression postoperatively, with only faint expression in select areas along the capsular border (Fig. 2D). By contrast, postoperative AR-Tg capsules showed even greater loss of E-cadherin expression in the cellular mass filling the capsular bag (Fig. 2F), displaying essentially background levels of staining. These data demonstrated that our mock cataract surgery procedure causes downregu-

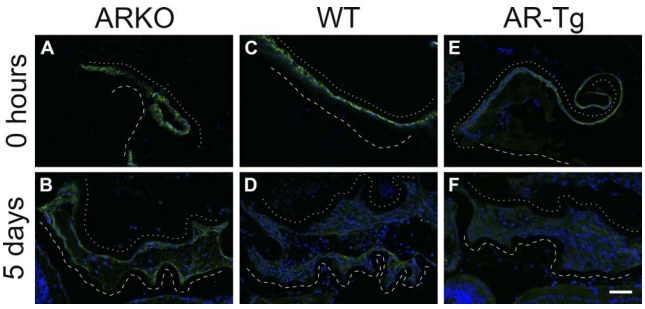

Figure 2. Expression of the lens epithelial cell marker E-cadherin 0 hours and 5 days after cataract surgery in ARKO (**A**, **B**), WT (**C**, **D**), and AR-Tg (**E**, **F**) mice. Immediately after surgery, E-cadherin expression is present in all strains (**A**, **C**, **E**), clearly visible between lens epithelial cells lining the anterior capsule. E-cadherin expression persists 5 days after surgery in ARKO (**B**), seen clearly between cells lining the anterior and posterior capsule. By contrast, no appreciable E-cadherin expression is seen 5 days postoperatively in WT (**D**) or AR-Tg (**F**). All panels show E-cadherin expression (*green*) along with nuclei (DAPI, *blue*). *Dotted line* traces the anterior capsule; dashed line traces the posterior capsule. *Scale bar*: 50 μm.

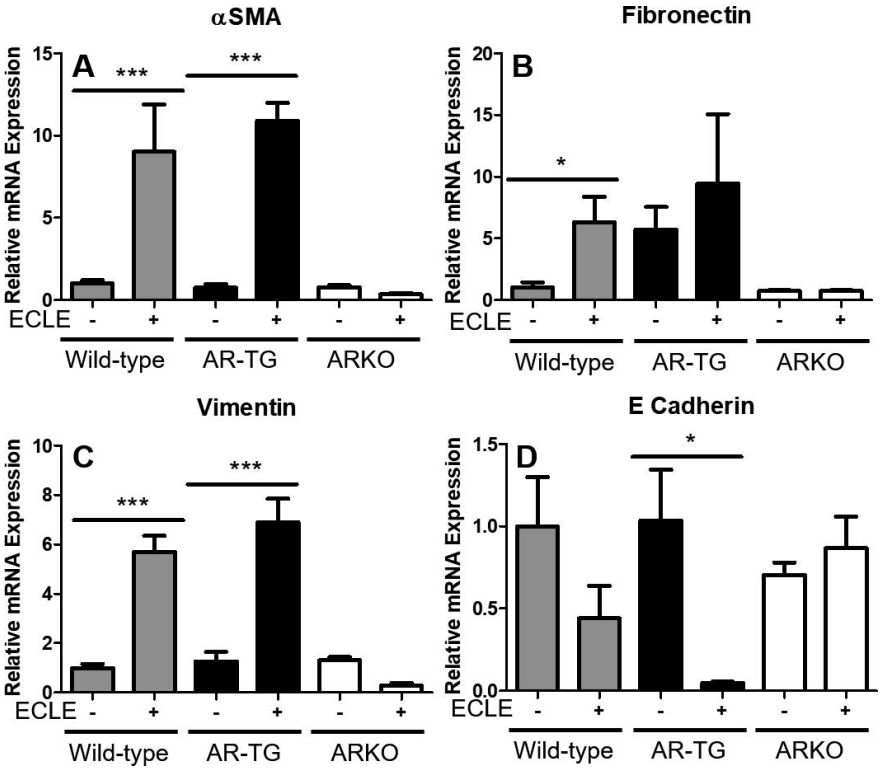

FIGURE 3. Genetic knockdown of AR prevents characteristic changes in EMT gene transcripts induced by ECLE. Messenger RNA was collected from dissected capsular bags 5 days after ECLE (or contralateral, unoperated eye within the same animal for controls). In both WT (*gray fill*) and AR-Tg (*black fill*), surgery induced increased expression of myofibroblast markers α-SMA (**A**), fibronectin (**B**), and vimentin (**C**), and a decrease in E-cadherin (**D**). However, these characteristic EMT changes were absent in ARKO (*white fill*) mice postoperatively. The data in each panel are normalized to the expression levels in WT without ECLE. Data are presented as mean ± SEM, with $n = 3$. $^{*}P < 0.05$, $^{**}P < 0.01$, $^{***}P < 0.001$.

lation of E-cadherin, but genetic AR knockout prevents this response and preserves expression of this epithelial marker.

Genetic Knockout of AR Prevents Characteristic EMT Changes in mRNA Levels Induced by Cataract Surgery

While the experiments above provide qualitative evidence that AR levels correlate positively with induction of EMT markers associated with PCO from a histologic perspective, we sought to confirm these results with quantitative measures of mRNA transcripts of EMT-related genes. To achieve this aim, we isolated RNA from postoperative capsular bags as well as contralateral capsular bags produced by ECLE at the time of euthanasia. In both WT and AR-Tg mice, we observed the expected changes in mRNA levels of informative genes associated with postoperative EMT. For example, capsular bags of WT and AR-Tg lenses contained markedly elevated transcript levels for α-SMA (Fig. 3A), fibronectin (Fig. 3B), and vimentin (Fig. 3C). The increase in AR-Tg fibronectin (Fig. 3B) did not reach statistical significance due to elevated baseline expression, consistent with our prior work with upstream EMT signaling mediators.[30] As expected, transcript levels for the epithelial marker E-cadherin were reduced in WT and AR-Tg lenses (Fig. 3D). Interestingly, E-cadherin reduction was more rapid and marked in AR-Tg than WT (which did not reach statistical significance 5 days postoperatively), suggesting a more robust EMT reaction. In contrast, in ARKO mice no significant changes in gene transcript levels of key markers of EMT were noted following ECLE in AR-deficient lenses (see ARKO in Figs. 3A–D). Thus, our surgical model induces a quantifiable change in EMT-related gene expression patterns that can be prevented through genetic knockout of AR.

Pharmacologic Suppression of AR Suppresses Characteristic EMT Changes in AR-Tg Mice After Cataract Surgery

Given that ECLE-induced PCO marker expression was lower in AR null mice, we sought to determine if treatment of animals with an AR inhibitor likewise protected against surgery-induced expression of PCO-related genes. Sorbinil is a well-established AR inhibitor shown to have effective penetration into ocular tissues.[36] We compared levels of EMT-related transcripts in postoperative eyes from mice treated with Sorbinil versus physiologic saline control (Fig. 4). In mice with low (WT) or null (ARKO) AR expression, Sorbinil treatment had negligible effects on ECLE-induced changes in αSMA (Fig. 4A), fibronectin (Fig. 4B), and vimentin (Fig. 4C) transcript levels. In contrast, in mice with relatively high levels of AR (AR-Tg), Sorbinil treatment significantly prevented ECLE-induced increases in gene transcripts from αSMA, fibronectin, and vimentin. Thus, pharmacological treatment with an AR inhibitor protected against surgery-induced upregulation of genes related to the EMT response in lens.

Genetic Knockout of AR Does Not Prevent the Postoperative Induction of the Lens Fiber Cell Marker αA-Crystallin

It is thought that incidental surgical trauma during cataract surgery leads to proliferation of remnant LECs along the posterior capsule[37] leading to two distinct histologic types of PCO: fibrotic PCO and pearl-type PCO.[38] Fibrotic PCO results

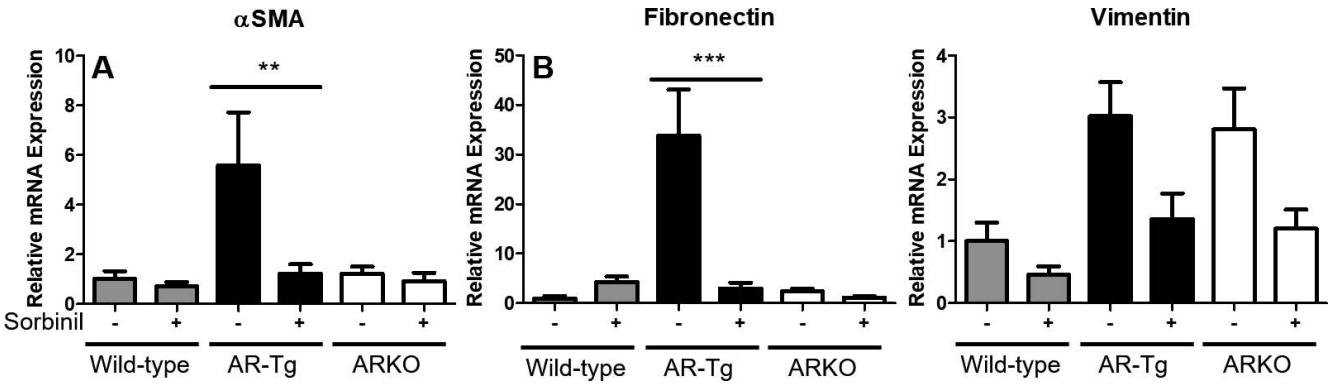

FIGURE 4. Pharmacologic inhibition of AR prevents characteristic changes in EMT gene transcripts induced by ECLE. Messenger RNA was collected from dissected capsular bags 5 days after ECLE. Of note, all data presented here comes from postoperative eyes, with controls receiving saline treatment and experimental animals receiving 10 mg/kg of Sorbinil intraperitoneally at the time of surgery and twice daily thereafter. While we did not observe significant effects from Sorbinil in WT (*gray fill*) mice, AR-Tg (*black fill*) postoperative eyes treated with the AR inhibitor demonstrated decreased expression of myofibroblast markers α-SMA (**A**), fibronectin (**B**), and vimentin (**C**). The data in each panel are normalized to the expression levels in postoperative WT without Sorbinil. Data are presented as mean ± SEM, with $n = 3$. $^{*}P < 0.05$, $^{**}P < 0.01$, $^{***}P < 0.001$.

from an EMT response in the remnant epithelial cells, which become myofibroblasts and express factors like α-SMA (as described above). Pearl-type PCO, by contrast, results from differentiation of epithelial cells into immature fiber cells, which are rich in crystallin proteins. Interestingly, both histologic variants can exist simultaneously within the same capsule and appear to come from a common response to cataract surgery.[39] Recently, experiments in cell culture have demonstrated that the known inducer of EMT and fibrotic PCO, TGF-β, is also a key inducer of the lens fiber cell response and pearl-type PCO.[40] With the data above demonstrating that AR inhibition can suppress post-cataract EMT and fibrotic PCO, we were motivated to investigate the influence of AR expression level on the pearl-type PCO response by immunostaining for the fiber cell markers αA-crystallin (Fig. 5) and Aquaporin 0 (AQP0, Fig. 6). Prior to surgery, αA-crystallin is known to be present diffusely throughout the lens in all mouse strains (data not shown).[41] Immediately following surgery, all strains exhibit αA-crystallin positivity in the remnant lenticular tissue, specifically the anterior lens epithelium (Figs. 5A, 5C, 5E). In both WT (Fig. 5D) and AR-Tg (Fig. 5F), abundant αA-crystallin is distributed throughout the capsular bag. In fact, the αA-crystallin distribution mirrors the α-SMA distribution we observed (Figs. 1D, 1F), consistent with the notion that both the fibrotic and pearl-type postoperative responses share a common trigger and coexist in the same capsule.[39] Interestingly, ARKO mice demonstrated a preserved pearl-type postoperative reaction, as evidenced by abundant αA-crystallin expression diffusely throughout the capsular bag (Fig. 5B). Immediate postoperative capsules contained little to no AQP0 (Figs. 6A, 6C, 6E), while all strains exhibited AQP0 positivity at 5 days (Figs. 6B, 6D, 6F). ARKO capsules displayed the most robust response (Fig. 6B), with AQP0 staining occupying a greater portion of the capsule compared to WT (Fig. 6D) and AR-Tg (Fig. 6F). In light of our observed minimal postoperative α-SMA expression in ARKO mice (Fig. 1B), this suggests that low levels of AR are associated with a reduced EMT and fibrotic PCO response, while at the same time preserving the pearl-type fiber cell response.

DISCUSSION

The world's leading cause of visual impairment is cataracts, causing 10.8 million cases of blindness and an additional 35.1

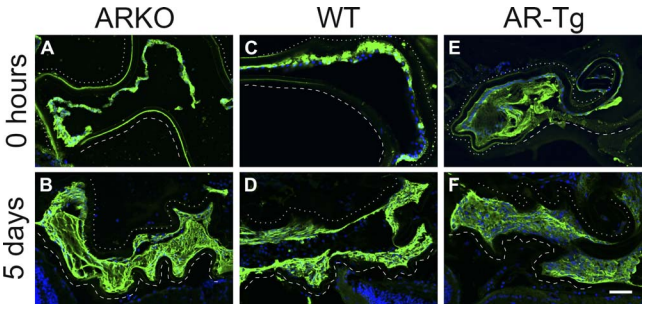

FIGURE 5. Expression of the lens fiber cell marker αA-crystallin 0 hours and 5 days after cataract surgery in ARKO (**A**, **B**), WT (**C**, **D**), and AR-Tg (**E**, **F**) mice. Immediately after surgery, αA-crystallin expression is present in all strains surrounding the lens epithelial cells lining the anterior capsular border (**A**, **C**, **E**). Five days postoperatively, αA-crystallin expression nearly fills the capsular bag space in all strains (**B**, **D**, **E**). Of note, in contrast to EMT markers, genetic knockdown of AR does not prevent induction of the lens fiber cell marker αA-crystallin postoperatively. All panels show αA-crystallin expression (*green*) along with nuclei (DAPI, *blue*). *Dotted line* traces the anterior capsule; dashed line traces the posterior capsule. *Scale bar*: 50 μm.

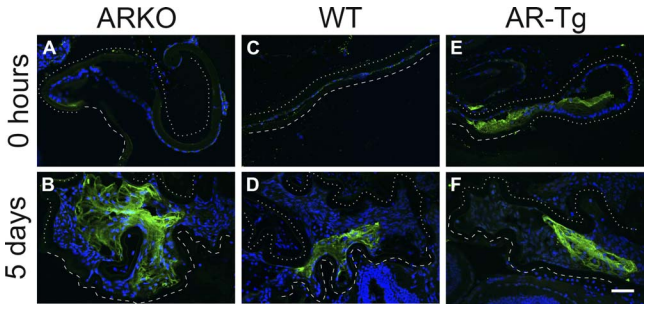

FIGURE 6. Expression of the lens fiber cell marker Aquaporin 0 (AQP0) 0 hours and 5 days after cataract surgery in ARKO (**A**, **B**), WT (**C**, **D**), and AR-Tg (**E**, **F**) mice. Immediately after surgery, little to no AQP0 expression is present in the capsules of all strains (**A**, **C**, **E**). Five days postoperatively, AQP0 expression fills a significant portion of the capsular bag space in ARKO (**B**), and a smaller region in WT (**D**) and AR-Tg (**F**). Of note, in contrast to EMT markers, genetic knockdown of AR does not prevent induction of the lens fiber cell marker AQP0 postoperatively. All panels show AQP0 expression (*green*) along with nuclei (DAPI, *blue*). Dotted line traces the anterior capsule; dashed line traces the posterior capsule. *Scale bar*: 50 μm.

million cases of visual impairment.[42] Accordingly, cataract surgery to remove the cloudy lens is among the most common surgical operations in the world. However, up to 20% to 30% of patients develop PCO postoperatively[1] usually requiring Nd:YAG laser capsulotomy to clear the visual axis. While YAG capsulotomy is generally considered safe, complications such as cystoid macular edema, secondary glaucoma, and retinal detachment are not unusual.[43,44] Furthermore, the economic burden of YAG capsulotomy is substantial—$158 million billed to Medicare in 2003[45]—which in turn limits its access in developing countries and other economically disadvantaged areas. Thus, not only is it important to understand the molecular mechanisms that control PCO, but prevention of PCO without the need of an additional laser procedure can positively impact millions globally, especially those with limited access to laser equipment in resource-poor areas.

It is thought that incidental surgical trauma during cataract surgery leads to proliferation of remnant LECs along the posterior capsule, leading to the clinical phenotype of PCO.[37] Despite decades of technical advances, it remains extremely difficult to remove all lens epithelial tissue during cataract surgery,[1,46,47] which can, in turn, undergo an aberrant wound-healing response resulting in PCO. TGF-β is known to be a key regulator of PCO through its role in inducing EMT in LECs.[2] The classic TGF-β signal transducers are SMAD proteins,[4–6,48] which lead to the formation of myofibroblast cells,[7] expression of various EMT markers,[8–12] and the histologic phenotype of fibrotic PCO.[38] Critically, it is known that TGF-β signaling increases in LECs that remain after cataract surgery,[6] representing a response to the mechanical trauma and injury of the procedure itself. TGF-β can also lead to another phenotype of PCO characterized by expression of lens fiber cell markers,[40] called pearl-type PCO,[38] through non-SMAD pathways.[49]

Another key regulator of PCO is aldose reductase (AR). Studied in-depth for its role in the ocular complications of diabetes, AR contributes to PCO through the production of ROS. Experimentation into AR signaling has demonstrated that AR contributes to ROS production,[15] ROS contributes to PCO,[16] AR inhibition suppresses ROS production in ocular tissues,[20–22] AR overexpression can induce PCO,[23] and AR inhibition can decrease markers of PCO.[24] Recently, we connected this extensive body of AR research with the large of body of knowledge about TGF-β by showing that AR inhibition prevents the markers of PCO by inhibiting TGF-β signaling.[21]

This present work extends previous cell culture and in vitro experiments and demonstrates that AR inhibition in an animal model of cataract surgery can suppress the histologic phenotype of fibrotic PCO. Through immunofluorescence and PCR, we showed that overexpression of AR results in a more robust induction of EMT after model cataract surgery, while genetic or pharmacologic AR inhibition significantly suppressed the cardinal manifestations of fibrotic PCO. With most prior research on AR and PCO employing cell culture models, this present work validates the hypothesis that AR inhibition can prevent PCO by using an in vivo animal model of surgery to display suppression of fibrotic PCO on a histologic level. Importantly, we recognize the limitation of our model to obtain reliable protein quantification due to extremely small tissue samples. Instead, we have combined corroborating mRNA and histologic evidence to support our conclusion.

As noted above, the postoperative induction of TGF-β can also lead to a pearl-type PCO, characterized by expression of lens fiber cell markers.[38,40,50] Both fibrotic and pearl-type PCO can coexist in the same postoperative capsule.[39] In this work, we demonstrate that not only do both of these processes coexist in the same capsule, but that both EMT and lens fiber differentiation are triggered simultaneously in response to surgery (Figs. 1D, 2D, 5D, 6D). Furthermore, we show that while AR inhibition effectively inhibits EMT, it does not prevent fiber cell differentiation and expression of the fiber cell markers αA-crystallin (Fig. 5B) and AQP0 (Fig. 6B). Taken together, these data represent the first example that this modified cataract surgical model can effectively trigger both types of PCO responses simultaneously and that AR inhibition can selectively inhibit EMT without abrogating fiber cell differentiation. It was recently shown that TGF-β triggers both pathways through different downstream pathways, including SMAD and non-SMAD cascades.[40,51,52] While we have demonstrated that AR inhibition prevented PCO and EMT markers through suppression of SMAD signaling,[21] AR activity has been shown to affect non-SMAD pathways as well.[53] Presumably, AR inhibition has less effect on those downstream pathways of TGF-β signaling that cause lens fiber cell differentiation, but this remains to be tested experimentally. Additionally, it is unknown whether AR inhibition can directly augment fiber cell differentiation or whether it simply shifts the biochemical equilibrium away from EMT, thereby increasing flux through the fiber cell pathway.

Acknowledgments

The authors thank Biehuoy Shieh for her help with maintaining the animal populations used in this study and Patricia Lenhart for her help with histopathology.

Supported in part by National Institutes of Health Grants EY005856 and EY028147 and by a Challenge Grant to the Department of Ophthalmology from Research to Prevent Blindness, Inc.

Disclosure: **L.M. Zukin**, None; **M.G. Pedler**, None; **S. Groman-Lupa**, None; **M. Pantcheva**, None; **D.A. Ammar**, None; **J.M. Petrash**, None

References

1. Awasthi N, Guo S, Wagner BJ. Posterior capsular opacification: a problem reduced but not yet eradicated. *Arch Ophthalmol*. 2009;127:555–562.
2. de Iongh RU, Wederell E, Lovicu FJ, McAvoy JW. Transforming growth factor-beta-induced epithelial-mesenchymal transition in the lens: a model for cataract formation. *Cells Tissues Organs*. 2005;179:43–55.
3. Nibourg LM, Gelens E, Kuijer R, Hooymans JMM, van Kooten TG, Koopmans SA. Prevention of posterior capsular opacification. *Exp Eye Res*. 2015;136:100–115.
4. Li J, Tang X, Chen X. Comparative effects of TGF-β2/Smad2 and TGF-β2/Smad3 signaling pathways on proliferation, migration, and extracellular matrix production in a human lens cell line. *Exp Eye Res*. 2011;92:173–179.
5. Wormstone IM, Tamiya S, Eldred JA, et al. Characterisation of TGF-beta2 signalling and function in a human lens cell line. *Exp Eye Res*. 2004;78:705–714.
6. Saika S, Miyamoto T, Ishida I, et al. TGFbeta-Smad signalling in postoperative human lens epithelial cells. *Br J Ophthalmol*. 2002;86:1428–1433.
7. Hales AM, Schulz MW, Chamberlain CG, McAvoy JW. TGF-beta 1 induces lens cells to accumulate alpha-smooth muscle actin, a marker for subcapsular cataracts. *Curr Eye Res*. 1994;13:885–890.
8. Wormstone IM, Tamiya S, Anderson I, Duncan G. TGF-beta2-induced matrix modification and cell transdifferentiation in the human lens capsular bag. *Invest Ophthalmol Vis Sci*. 2002;43:2301–2308.
9. Saika S, Kawashima Y, Miyamoto T, et al. Immunolocalization of prolyl 4-hydroxylase subunits, alpha-smooth muscle actin,

and extracellular matrix components in human lens capsules with lens implants. *Exp Eye Res*. 1998;66:283–294.

10. Azuma N, Hara T, Hara T. Extracellular matrix of opacified anterior capsule after endocapsular cataract surgery. *Graefes Arch Clin Exp Ophthalmol*. 1998;236:531–536.
11. Marcantonio JM, Syam PP, Liu CSC, Duncan G. Epithelial transdifferentiation and cataract in the human lens. *Exp Eye Res*. 2003;77:339–346.
12. Liu J, Hales AM, Chamberlain CG, McAvoy JW. Induction of cataract-like changes in rat lens epithelial explants by transforming growth factor beta. *Invest Ophthalmol Vis Sci*. 1994;35:388–401.
13. Hales AM, Chamberlain CG, McAvoy JW. Cataract induction in lenses cultured with transforming growth factor-beta. *Invest Ophthalmol Vis Sci*. 1995;36:1709–1713.
14. Wang Y, Li W, Zang X, et al. MicroRNA-204-5p regulates epithelial-to-mesenchymal transition during human posterior capsule opacification by targeting SMAD4. *Invest Ophthalmol Vis Sci*. 2013;54:323–332.
15. Tang WH, Martin KA, Hwa J. Aldose reductase, oxidative stress, and diabetic mellitus. *Front Pharmacol*. 2012;3:87.
16. Chen KC-W, Zhou Y, Zhang W, Lou MF. Control of PDGF-induced reactive oxygen species (ROS) generation and signal transduction in human lens epithelial cells. *Mol Vis*. 2007;13:374–387.
17. Hepsen IF, Bayramlar H, Gultek A, Ozen S, Tilgen F, Evereklioglu C. Caffeic acid phenethyl ester to inhibit posterior capsule opacification in rabbits. *J Cataract Refract Surg*. 1997;23:1572–1576.
18. Doganay S, Turkoz Y, Evereklioglu C, Er H, Bozaran M, Ozerol E. Use of caffeic acid phenethyl ester to prevent sodium-selenite-induced cataract in rat eyes. *J Cataract Refract Surg*. 2002;28:1457–1462.
19. Inan UU, Oztürk F, Kaynak S, et al. Prevention of posterior capsule opacification by intraoperative single-dose pharmacologic agents. *J Cataract Refract Surg*. 2001;27:1079–1087.
20. Chang K-C, Laffin B, Ponder J, et al. Beta-glucogallin reduces the expression of lipopolysaccharide-induced inflammatory markers by inhibition of aldose reductase in murine macrophages and ocular tissues. *Chem Biol Interact*. 2013;202:283–287.
21. Chang K-C, Petrash JM. Aldose reductase mediates transforming growth factor β2 (TGF-β2)-induced migration and epithelial-to-mesenchymal transition of lens-derived epithelial cells. *Invest Ophthalmol Vis Sci*. 2015;56:4198–4210.
22. Ramana KV, Fadl AA, Tammali R, Reddy ABM, Chopra AK, Srivastava SK. Aldose reductase mediates the lipopolysaccharide-induced release of inflammatory mediators in RAW264.7 murine macrophages. *J Biol Chem*. 2006;281:33019–33029.
23. Zablocki GJ, Ruzycki PA, Overturf MA, Palla S, Reddy GB, Petrash JM. Aldose reductase-mediated induction of epithelium-to-mesenchymal transition (EMT) in lens. *Chem Biol Interact*. 2011;191:351–356.
24. Yadav UC, Ighani-Hosseinabad F, van Kuijk FJGM, Srivastava SK, Ramana KV. Prevention of posterior capsular opacification through aldose reductase inhibition. *Invest Ophthalmol Vis Sci*. 2009;50:752–759.
25. Zenon GJ, Abobo CV, Carter BL, Ball DW. Potential use of aldose reductase inhibitors to prevent diabetic complications. *Clin Pharm*. 1990;9:446–457.
26. Lee AY, Chung SS. Contributions of polyol pathway to oxidative stress in diabetic cataract. *FASEB J*. 1999;13:23–30.
27. Srivastava SK, Ramana KV, Bhatnagar A. Role of aldose reductase and oxidative damage in diabetes and the consequent potential for therapeutic options. *Endocr Rev*. 2005;26:380–392.
28. Wormstone IM, Eldred JA. Experimental models for posterior capsule opacification research. *Exp Eye Res*. 2016;142:2–12.
29. Chang K-C, Shieh B, Petrash JM. Influence of aldose reductase on epithelial-to-mesenchymal transition signaling in lens epithelial cells. *Chem Biol Interact*. 2017;276:149–154.
30. Snow A, Shieh B, Chang K-C, et al. Aldose reductase expression as a risk factor for cataract. *Chem Biol Interact*. 2015;234:247–253.
31. Ho HT, Chung SK, Law JW, et al. Aldose reductase-deficient mice develop nephrogenic diabetes insipidus. *Mol Cell Biol*. 2000;20:5840–5846.
32. Mamuya FA, Wang Y, Roop VH, Scheiblin DA, Zajac JC, Duncan MK. The roles of alphaV integrins in lens EMT and posterior capsular opacification. *J Cell Mol Med*. 2014;18:656–670.
33. Desai VD, Wang Y, Simirskii VN, Duncan MK. CD44 expression is developmentally regulated in the mouse lens and increases in the lens epithelium after injury. *Differentiation*. 2010;79:111–119.
34. Call MK, Grogg MW, Del Rio-Tsonis K, Tsonis PA. Lens regeneration in mice: implications in cataracts. *Exp Eye Res*. 2004;78:297–299.
35. Kalluri R, Weinberg RA. The basics of epithelial-mesenchymal transition. *J Clin Invest*. 2009;119:1420–1428.
36. Crabbe MJ, Petchey M, Burgess SE, Cheng H. The penetration of Sorbinil, an aldose reductase inhibitor, into lens, aqueous humour and erythrocytes of patients undergoing cataract extraction. *Exp Eye Res*. 1985;40:95–99.
37. Petrash JM. Aging and age-related diseases of the ocular lens and vitreous body. *Invest Ophthalmol Vis Sci*. 2013;54:ORSF54–59.
38. Apple DJ, Solomon KD, Tetz MR, et al. Posterior capsule opacification. *Surv Ophthalmol*. 1992;37:73–116.
39. Raj SM, Vasavada AR, Johar SRK, Vasavada VA, Vasavada VA. Post-operative capsular opacification: a review. *Int J Biomed Sci*. 2007;3:237–250.
40. Boswell BA, Korol A, West-Mays JA, Musil LS. Dual function of TGFβ in lens epithelial cell fate: implications for secondary cataract. *Mol Biol Cell*. 2017;28:907–921.
41. Wen Y, Shi ST, Unakar NJ, Bekhor I. Crystallin mRNA concentrations and distribution in lens of normal and galactosemic rats. Implications in development of sugar cataracts. *Invest Ophthalmol Vis Sci*. 1991;32:1638–1647.
42. Khairallah M, Kahloun R, Bourne R, et al. Number of people blind or visually impaired by cataract worldwide and in world regions, 1990 to 2010. *Invest Ophthalmol Vis Sci*. 2015;56:6762–6769.
43. Javitt JC, Tielsch JM, Canner JK, Kolb MM, Sommer A, Steinberg EP; The Cataract Patient Outcomes Research Team. National outcomes of cataract extraction. Increased risk of retinal complications associated with Nd:YAG laser capsulotomy. *Ophthalmology*. 1992;99:1487–1497; discussion,1497–1498.
44. Pandey SK, Apple DJ, Werner L, Maloof AJ, Milverton EJ. Posterior capsule opacification: a review of the aetiopathogenesis, experimental and clinical studies and factors for prevention. *Indian J Ophthalmol*. 2004;52:99–112.
45. Cleary G, Spalton DJ, Koch DD. Effect of square-edged intraocular lenses on neodymium:YAG laser capsulotomy rates in the United States. *J Cataract Refract Surg*. 2007;33:1899–1906.
46. Wormstone IM, Wang L, Liu CSC. Posterior capsule opacification. *Exp Eye Res*. 2009;88:257–269.
47. Apple DJ, Escobar-Gomez M, Zaugg B, Kleinmann G, Borkenstein AF. Modern cataract surgery: unfinished business and unanswered questions. *Surv Ophthalmol*. 2011;56(suppl 6):S3–S53.
48. Li H, Yuan X, Li J, Tang X. Implication of Smad2 and Smad3 in transforming growth factor-β-induced posterior capsular

opacification of human lens epithelial cells. *Curr Eye Res*. 2015;40:386–397.

49. Zhang YE. Non-Smad pathways in TGF-beta signaling. *Cell Res*. 2009;19:128–139.
50. Lovicu FJ, Shin EH, McAvoy JW. Fibrosis in the lens. Sprouty regulation of TGFβ-signaling prevents lens EMT leading to cataract. *Exp Eye Res*. 2016;142:92–101.
51. Lovicu FJ, Steven P, Saika S, McAvoy JW. Aberrant lens fiber differentiation in anterior subcapsular cataract formation: a process dependent on reduced levels of Pax6. *Invest Ophthalmol Vis Sci*. 2004;45:1946–1953.
52. Banh A, Deschamps PA, Gauldie J, et al. Lens-specific expression of TGF-β induces anterior subcapsular cataract formation in the absence of Smad3. *Invest Ophthalmol Vis Sci*. 2006;47:3450–3460.
53. Chang KC, Shieh B, Petrash JM. Influence of aldose reductase on epithelial-to-mesenchymal transition signaling in lens epithelial cells. *Chem Biol Interact*. 2017;276:149–154.

Investigative Ophthalmology & Visual Science